

# Meta-Transfer Networks for Zero-Shot Learning

Yunlong Yu  
Zhejiang University  
yuyunlong@zju.edu.cn

Zhongfei Zhang  
Binghamton University  
zhongfei@cs.binghamton.edu

Jungong Han  
The University of Warwick  
jungong.han@warwick.ac.uk

## Abstract

*Zero-Shot Learning (ZSL) aims at recognizing unseen categories using some class semantics of the categories. The existing studies mostly leverage the seen categories to learn a visual-semantic interaction model to infer the unseen categories. However, the disjointness between the seen and unseen categories cannot ensure that the models trained on the seen categories generalize well to the unseen categories. In this work, we propose an episode-based approach to accumulate experiences on addressing disjointness issue by mimicking extensive classification scenarios where training classes and test classes are disjoint. In each episode, a visual-semantic interaction model is first trained on a subset of seen categories as a learner that provides an initial prediction for the rest disjoint seen categories and then a meta-learner fine-tunes the learner by minimizing the differences between the prediction and the ground-truth labels in a pre-defined space. By training extensive episodes on the seen categories, the model is trained to be an expert in predicting the mimetic unseen categories, which will generalize well to the real unseen categories. Extensive experiments on four datasets under both the traditional ZSL and generalized ZSL tasks show that our framework outperforms the state-of-the-art approaches by large margins.*

## 1. Introduction

With the recent renaissance of deep learning, tremendous breakthroughs have been achieved on various visual tasks. However, the deep learning techniques predominantly rely on the availability of artificially balanced training data, which poses a significant bottleneck against building comprehensive models for the real visual world. In recent years, Zero-Shot Learning [11, 31, 32] has been attracting a lot of attention due to its potential to address the data scarcity issue.

Zero-Shot Learning (ZSL) aims at recognizing unseen classes that have no visual instances during the training stage. Such a harsh but realistic scenario is painful for the

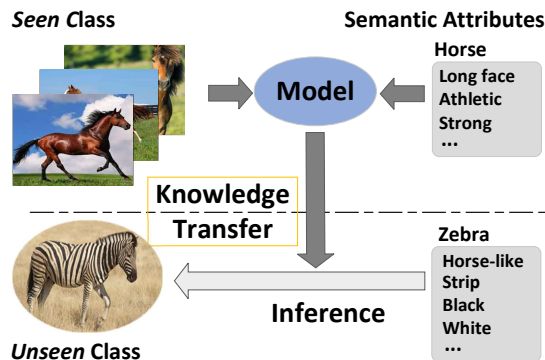


Figure 1. The basic framework of the existing ZSL approaches, which trains a model to construct the visual-semantic interaction with the seen data and generalizes it to the unseen data.

traditional classification approaches because there is no labeled visual data to support the parameters training. ZSL methods address this problem by leveraging the seen classes that have abundant visual data to learn a visual-semantic interaction model, which can be in turn used to infer unseen visual instances from their corresponding class semantics, as illustrated in Fig. 1.

Although promising performances have been achieved, the existing approaches mostly dedicate to designing visual-semantic interaction models with the seen classes, which cannot ensure that they generalize well to the unseen classes as the seen and unseen classes are literally disjoint. Inspired by the success of meta-learning in the few-shot learning task, we propose an episode-based framework that trains a specific model for unseen classes. Specifically, each episode mimics a zero-shot learning task, of which the training classes and the test classes are disjoint. In each episode, the seen classes are randomly split into two disjoint class sets, one training set, and one test set. The training set is taken as input to train a learner, which is a parameterized function that builds semantic interactions between the visual and the class semantic modalities by minimizing the semantic differences across different modalities. Meta-learner is trained by feeding the test set to the learner to obtain the initialized label prediction and then to fine-tune the learner by minimizing the difference between the prediction and the

ground-truth in a pre-defined space. By training extensive episodes in the seen data, the model accumulates ensemble experiences on predicting unseen categories, which is trained to be an expert for zero-shot learning.

Under the meta-learning framework, we propose a novel approach called **Meta-Transfer Network (MTN)** that leverages the merits of both the transfer learning and meta-learning paradigm. The learner in the **MTN** is a well-designed semantic-visual interaction network, which interweaves both the visual features and the class semantic features tightly to align the cross-modal semantics and capture discriminative information. Specifically, both the visual features and class semantic features are fed into a cycle network to align the semantic consistency with an adversarial loss. To effectively capture the discriminative information, we devise a novel **Multi-modal Cross-Entropy Loss** to integrate both the visual features, class semantic features, and class labels into a classification network. With the trained learner, each class semantic vector obtains its corresponding visual prototype in the visual space. The meta-learner in the **MTN** feeds both the mimetic unseen visual data and their corresponding class semantic vectors into the learner to obtain the initialized prediction based on the similarities between the unseen visual data and class visual prototypes with a specific distance metric. By minimizing the differences between the prediction and ground-truth labels, the meta-learner fine-tunes the parameters of the learner to encourage the learner to be suited for the unseen classes.

In summary, our contributions are concluded into the following three-fold.

1. We introduce an episode-based paradigm to address zero-shot learning, where each episode mimics a specific zero-shot learning task. By training extensive episodes, the model accumulates a wealth of experiences on predicting the mimetic unseen classes, which will generalize well to the real unseen classes.
2. We propose a well-designed network to construct the visual-semantic interactions, which consists of a cycle network to align the semantic consistency across different modalities and an effective classification network to capture the discriminative information with a novel **Multi-modal Cross-Entropy Loss**.
3. Extensive experiments on four benchmark datasets show that the proposed approach achieves state-of-the-art performances under both the traditional ZSL and realistic generalized ZSL evaluation protocols.

## 2. Related Work

In this section, we provide an overview of the most related work on zero-shot learning and meta-learning approaches.

### 2.1. Zero-Shot Learning

Over the past years, a large number of ZSL approaches have been proposed. Most approaches directly train an interaction model to align the semantic consistency between the visual and the class semantic modalities. Based on the way of modeling, the existing approaches can be roughly divided into discriminative approaches and generative approaches. The discriminative approaches either train a projection function to map the visual features into the class semantic space [14, 21] or learn a compatibility function to evaluate the semantic similarity between the visual features and the class semantic features [6, 1, 2, 18, 33] with different losses. [19] demonstrates that the methods that project the high-dimensional visual features into a low-dimensional class semantic space easily suffer from “hubness” issue that the tendency of some unseen class prototypes (“hubs”) appearing in the top neighbors of many test instances, which will damage the classification performances. To address this issue, the generative approaches are proposed one after another. In contrast to the discriminative approaches, the generative approaches learn an inverse projection function that maps the class semantic features into the visual space. For example, DEM [34] directly trains a three-layer neural network to project the class semantic features into the visual space. Motivated by the success of generative adversarial network (GAN) [7, 3] and variational autoencoder (VAE) [9], the generative approaches tend to be the mainstream to address zero-shot learning task. [28, 35, 30, 12] leverage GAN to regularize the distribution differences between the generated visual features and the real visual features, while [25] uses VAE to fit the class-specific latent distribution and highly discriminative feature representations.

The models trained only with the seen classes tend to generalize modestly on the unseen classes due to their disjointness, resulting in the domain shift issue. In contrast, our approach boosts the generalized ability to unseen classes by accumulating ensemble experiences on addressing the disjoint classification tasks with an episode-based paradigm.

### 2.2. Meta-Learning

Meta-learning, also called learning to learn, attracts a lot of attention in few-shot learning task [16, 20, 5]. It formulates the training process into extensive episodes on the labeled examples of base categories, each of which mimics a few-shot learning task. The existing meta-learning algorithms for few-shot learning can be divided into three categories: model-based, metric-based, and optimization based approaches. The model-based approaches [15, 26] devise the models to fit the classification parameters with a few samples. The metric-based approaches [23, 20] aim to learn a metric space to evaluate the similarities between different samples. Optimization-based approaches [16, 5]

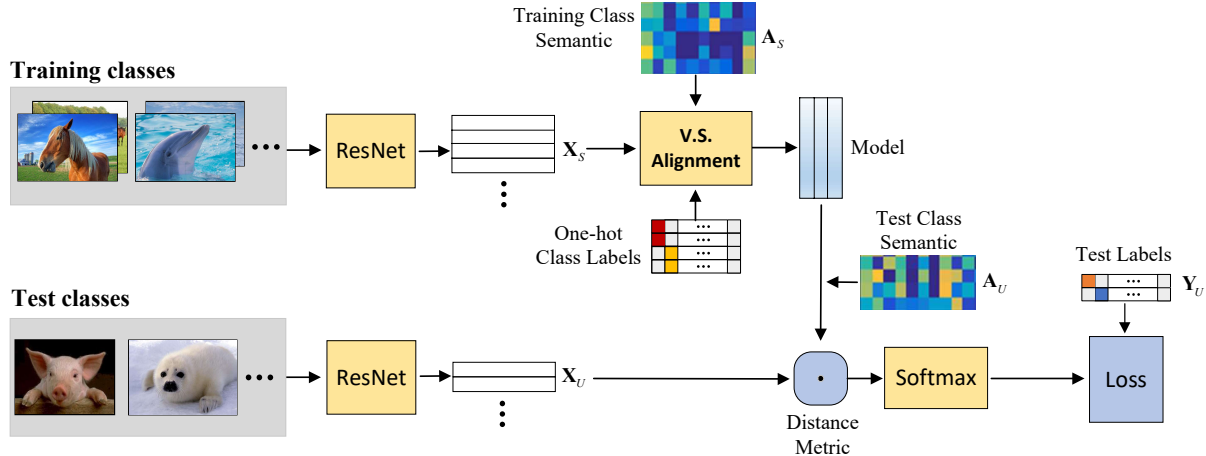


Figure 2. Diagram of the proposed method for one episode (task). The learner leverages the training classes to train a model by constructing the visual-semantic alignment (V.S. Alignment) across the visual and class semantic modalities. The meta-learner first initializes the label prediction of the unseen test data with the trained model in a pre-defined space and then fine-tunes the learner by minimizing the differences between the predicted results and the ground-truth labels.

assume that the model trained with traditional gradient decent approaches could not converge with a few samples, and learn a desired initial state, where the models could converge within a few optimization steps.

In this work, we also apply episode-based paradigm to train the transfer model. Differently, each episode in our approach mimics a zero-shot learning task, which requires to train a visual-semantic interaction model to achieve the knowledge transfer. One related work to ours is RELATION NETWORK [22] that also trains a zero-shot learning model in an episode-based paradigm. However, RELATION NETWORK [22] learns a metric space to evaluate the relations between the visual instances and the class semantic features rather than simulating zero-shot learning task.

### 3. Methodology

#### 3.1. Problem Formulation

The zero-shot classification task aims at inferring unseen categories with the corresponding class semantics. To achieve this task, a basic inferential criterion from the class semantics to visual samples should be learned with some seen categories. Suppose we collect  $N$  samples  $\{\mathbf{x}_i, \mathbf{a}_i, \mathbf{y}_i\}_{i=1}^N$  from  $M$  seen categories, where  $\mathbf{x}_i \in \mathbb{R}^D$  is the  $D$ -dimensional visual representation (e.g., CNN feature) for the  $i$ -th instance,  $\mathbf{a}_i \in \mathbb{R}^K$  and  $\mathbf{y}_i$  are its  $K$ -dimensional class semantic vector and one-hot class label, respectively. In the test stage, the task is to classify the test instance  $\mathbf{x}_t$  into the correct unseen categories on the condition that the class semantics  $\mathbf{A}_T \in \mathbb{R}^{K \times R}$  are provided, where  $R$  is the number of unseen categories.

In the training stage, we introduce the episode-based paradigm for training, which trains the model by mimick-

ing extensive zero-shot tasks on the seen categories. For each episode, the seen categories are randomly subdivided into two disjoint sets, one training set  $\mathcal{S} = \{\mathbf{X}_S, \mathbf{A}_S, \mathbf{Y}_S\}$  and one test set  $\mathcal{U} = \{\mathbf{X}_U, \mathbf{A}_U, \mathbf{Y}_U\}$ , where  $\mathbf{Y}_S$  and  $\mathbf{Y}_U$  are disjoint.

#### 3.2. Model

As illustrated in Fig. 2, each episode consists of a training stage as a learner and a test stage as a meta-learner. The training stage aims at learning a visual-semantic interaction model to align the semantic consistency, which can be used to predict the unseen categories from the class semantics. The test stage updates the parameters of the trained model by minimizing the predicted results and the ground-truth labels. Training each episode can be seen as a process of accumulating experience on zero-shot classification. After training extensive episodes, the model is expected to be an expert in predicting unseen categories, i.e., zero-shot learning.

##### 3.2.1 Learner.

The learner aims at learning a criterion to infer unseen categories from the corresponding class semantics. Similar with the exiting approaches, we also train an interaction model to align the semantic consistency across different modalities. Specifically, we devise a novel cycle embedding network to achieve this goal.

For the visual modality, we try to learn a mapping function  $f : \mathbb{R}^D \rightarrow \mathbb{R}^K$  to project the image features into the class semantic space by encouraging the image features to be close to the corresponding class semantic vectors, which

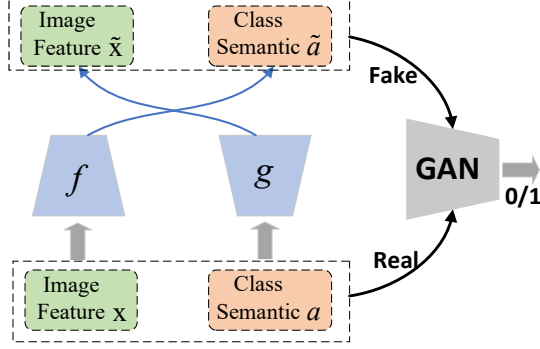


Figure 3. The basic model that aligns the semantic consistency across different modalities. The combination of both image feature  $\mathbf{x}$  and class semantic vector  $\mathbf{a}$  takes as the real input, while the combination of both the generated visual feature  $\tilde{\mathbf{x}}$  and the projected class semantic vector  $\tilde{\mathbf{a}}$  as the fake input of the discriminator  $D$ .

can be formulated as:

$$L_{\mathcal{V} \rightarrow \mathcal{A}} = \sum_i \|f(\mathbf{x}_i) - \mathbf{a}_i\|_2^2. \quad (1)$$

Similarly, for the class semantic modality, we try to learn another mapping function  $g : \mathbb{R}^K \rightarrow \mathbb{R}^D$  to project the class semantics into the visual space. Since each class usually consists of many image examples while corresponds to only one class semantic vector, the mapping function  $g$  can be seen as a one-to-many semantic-to-visual feature generator. The mapping function  $g$  is learned by minimizing the distances between the generated visual feature  $g(\mathbf{a}_i)$  and the real visual feature  $\mathbf{x}_i$ .

$$L_{\mathcal{A} \rightarrow \mathcal{V}} = \sum_i \|g(\mathbf{a}_i) - \mathbf{x}_i\|_2^2. \quad (2)$$

With the two mapping functions  $f$  and  $g$ , we can construct the relationships between the visual space and the class semantic space. However, they are independent to each other. To better align the semantic consistency, we introduce the adversarial mechanism to regularize both two mapping networks, as illustrated in Fig. 3. Specifically, we leverage the improved WGAN [8] to integrate the projected class semantic vector  $\tilde{\mathbf{a}}$  and the real class semantic vector  $\mathbf{a}$  separately to generator and discriminator. The loss is written:

$$L_{WGAN} = \mathbb{E}[D(\mathbf{x}, \mathbf{a})] - \mathbb{E}[D(\tilde{\mathbf{x}}, \tilde{\mathbf{a}})] - \lambda \mathbb{E}[(\|\nabla_{\tilde{\mathbf{x}}} D(\tilde{\mathbf{x}}, \tilde{\mathbf{a}})\|_2 - 1)^2], \quad (3)$$

where  $\tilde{\mathbf{a}} = f(\mathbf{x})$  is the projected class semantic vector;  $\tilde{\mathbf{x}} = g(\mathbf{a})$  is the generated visual feature.  $\hat{\mathbf{x}} = \alpha \mathbf{x} + (1 - \alpha)\tilde{\mathbf{x}}$  and  $\hat{\mathbf{a}} = \alpha \mathbf{a} + (1 - \alpha)\tilde{\mathbf{a}}$  with  $\alpha \sim U(0, 1)$ , and  $\lambda$  is the penalty coefficient. The discriminator  $D$  is a three-layer neural network. The above model aligns the semantic consistency between the visual features and class semantics. However,

training such a model neglects to exploit the discriminative information to distinguish categories, which is essential to the final class prediction. To address this issue, we propose a multi-modal cross-entropy loss that interweaves the image features, class semantics, and the one-hot class labels into a united framework. Intuitively, the visual features from the same category are required to have higher affinities with their corresponding class semantic vector than the other class semantic vectors. The multi-modal affinity is calculated as the inner products of the features from the two modalities. In the visual space, class semantic features of all training categories are projected into the corresponding class visual prototypes that are pre-stored in a visual feature buffer  $g(\mathbf{A}_S)$ , where  $g(\mathbf{a}_i)$  denotes the class visual prototype of  $i$ -th category. The affinities between a visual sample  $\mathbf{x}$  and all class visual prototypes could be obtained as  $\mathbf{x}^T g(\mathbf{A}_S)$ . In this way, the probability of the input visual sample  $\mathbf{x}$  belonging to the  $i$ -th category in the visual space can be evaluated with the affinity of visual sample  $\mathbf{x}$  matching the  $i$ -th class semantic vector with the following cross-modal softmax function:

$$p_i^{\mathcal{V}}(\mathbf{x}) = \frac{\exp(\mathbf{x}^T g(\mathbf{a}_i))}{\sum_j \exp(\mathbf{x}^T g(\mathbf{a}_j))}. \quad (4)$$

Similarly, in the class semantic space, all class semantic vectors are pre-stored in a class semantic buffer  $\mathbf{A}_S$  and a visual sample  $\mathbf{x}$  is represented as  $f(\mathbf{x})$  with the mapping function  $f$ . Therefore, the probability of  $\mathbf{x}$  belongs to the  $i$ -th category in the class semantic space is defined as

$$p_i^{\mathcal{S}}(\mathbf{x}) = \frac{\exp(f(\mathbf{x})^T \mathbf{a}_i)}{\sum_j \exp(f(\mathbf{x})^T \mathbf{a}_j)}. \quad (5)$$

Our goal is to maximize the above probabilities in both visual and class semantic space, which can be formulated by minimizing the following loss,

$$L_{MCE} = - \sum_{\mathbf{x}} \log p_i^{\mathcal{V}}(\mathbf{x}) - \sum_{\mathbf{x}} \log p_i^{\mathcal{S}}(\mathbf{x}). \quad (6)$$

Compared with the existing generative approaches [28, 12] that train a softmax classification model with both the real seen visual features and the generated unseen visual features, our classification model introduces no extra parameters, which is more efficient and feasible.

Overall, our full objective then becomes,

$$\min_g \max_D L_{WGAN} + L_{\mathcal{V} \rightarrow \mathcal{A}} + L_{\mathcal{A} \rightarrow \mathcal{V}} + L_{MCE}. \quad (7)$$

### 3.3. Meta-learner.

With the trained mapping functions  $f$  and  $g$ , the unseen instances could be predicted by applying the nearest neighbor classifier on the similarities between the visual instances

and the unseen class semantics in a same space. To alleviate the ‘‘hubness’’ issue, we also project the low-dimensional class semantics into the high-dimensional visual space and calculate the similarities with a pre-defined distance metric. For an unseen instance  $\mathbf{x}_t$ , its class label is predicted by,

$$\hat{y}_t = \arg \min_k (d(\mathbf{x}_t, g(\mathbf{a}_k))), \quad (8)$$

where  $\mathbf{a}_k$  is the class semantic vector of the  $k$ -th unseen category.  $d(\cdot, \cdot)$  denotes a certain distance metric, such as Euclidean or Cosine distance.

The model trained in the learner focuses on aligning the semantic consistency on the seen categories, which cannot ensure that it generalizes well to the unseen categories in the pre-defined metric space. To better transfer the learned knowledge to the unseen categories, we train a meta-learner on the unseen set  $\mathcal{U}$  to refine the learner to adapt the unseen categories in the pre-defined metric space. Given a distance function  $d$ , the meta-learner produces a distribution over classes for a test instance  $\mathbf{x}_t$  based on a softmax over distance to the class semantics in the visual space,

$$p_g(y = k | \mathbf{x}_t) = \frac{\exp(-d(\mathbf{x}_t, g(\mathbf{a}_k)))}{\sum_{k'} \exp(-d(\mathbf{x}_t, g(\mathbf{a}_{k'})))}. \quad (9)$$

$d(\cdot, \cdot)$  is the distance metric same as in Eq. (8). By minimizing the negative log-probability  $J(g) = -\log p_g(y = k | \mathbf{x}_t)$  of the true class  $k$ , the mapping function  $g$  is improved for generalizing unseen categories in the defined metric space. We observe empirically that the choice of distance metric is vital, as the classification performances with Euclidean distance mostly outperforms those with Cosine distance metric. In the experiments, we report the results with Euclidean distance, if not specific.

## 4. Experiments

In this section, we evaluate our proposed approach on both traditional ZSL and the challenging generalized ZSL tasks. First, we briefly document the datasets and experimental settings. Then, we compare our proposed MTN with the state-of-the-art. Additionally, we conduct further studies to evaluate the effects of the episode-based training paradigm and the distance metric for the classification.

### 4.1. Datasets and Experimental settings

#### 4.1.1 Datasets.

We evaluate our model on the four benchmark datasets, namely Animals with Attributes (AwA1) [11], Animals with Attributes2 (AwA2) [29], Caltech-UCSD Birds-200-2011 (CUB) [24], and Oxford Flowers (FLO) [13]. Both AwA1 and AwA2 are two coarse-grained datasets consisting of different visual images from the same 50 classes,

Table 1. The statistic of four benchmark datasets, in terms of dimensionality of class semantic  $sem$ , number of seen classes  $\mathcal{Y}_s$ , number of unseen classes  $\mathcal{Y}_u$ , number of all instances  $\mathcal{X}_a$ , number of test seen instances  $\mathcal{X}_s$  and unseen instances  $\mathcal{X}_u$ .

Dataset	$sem$	$\mathcal{Y}_s$	$\mathcal{Y}_u$	$\mathcal{X}_a$	$\mathcal{X}_s$	$\mathcal{X}_u$
AwA1	85	40	10	30,475	5,685	4,958
AwA2	85	40	10	37,322	5,882	7,913
CUB	1,024	150	50	11,788	2,967	1,764
FLO	1,024	82	20	8,189	5,394	1,155

each class is annotated with 85-dimensional semantic attributes. Specifically, AwA1 contains 30,475 instances while AwA2 contains the different 37,322 visual images. Both CUB and FLO are fine-grained image datasets that contain 200 bird species and 102 flower categories, respectively. As for the class semantic representations of both CUB and FLO datasets, we extract 1,024-dimensional character-based CNN-RNN [17] features from the fine-grained visual descriptions (10 sentences per image). We use the standard zero-shot splits provided by [29] for AwA1, AwA2, and CUB datasets. For FLO dataset, we use the splits provided by [13]. A dataset summary is given in Table 1.

#### 4.1.2 Implemental settings.

Following [29, 28], we use the 2,048-dimensional top pooling units of a ResNet-101 pretrained on ImageNet-1K as the image features. As a pre-processing step, we normalize the visual features into  $[0,1]$ . As for the class semantic embeddings, no pre-processing is applied. In the learner, both the mapping function  $f$  and  $g$  are three-layer neural networks whose hidden layer has 1,800 hidden units. In each episode, five random categories are split from the seen classes as the test unseen classes and the Euclidean distance is used as the measure metric. During training, we use the Adam optimizer with learning rate  $10^{-4}$ .

## 4.2. Experimental Results

### 4.2.1 Results on traditional ZSL.

Under the traditional ZSL setting, the test instances are classified into the unseen classes. To balance the prediction accuracy across all classes, we measure the average per-class top-1 accuracy (**T**) as the evaluation protocol. We compare our approach with twelve competitors including five discriminative approaches, six generative approaches, and one episode-based approach. The comparison results are reported in Table 2.

From Table 2, we observe that the proposed MTN achieves the state-of-the-art performances on four datasets. In specific, the overall accuracy improvement on AwA1 is from 71.1% to 74.3%, on AwA2 from 70.4% to 72.8%, on

Table 2. Traditional ZSL results on the four benchmark datasets. The results report average per-class top-1 accuracy (%). The best-performing performances are marked with the bold font on all datasets. \* indicates the result obtained by ourselves with the codes released by the authors.

Method	Dataset			
	AwA1	AwA2	CUB	FLO
DEVISE [6]	54.2	59.7	52.0	45.9
ALE [1]	59.9	62.5	54.9	48.5
ESZSL [18]	58.2	58.6	53.9	51.0
SJE [2]	65.6	61.9	53.9	53.4
LATEM [27]	55.1	55.8	49.3	40.4
GAZSL [35]	68.2	70.2	55.8	60.5
CLSWGAN [28]	68.2	65.3	57.3	67.2
SE-ZSL [10]	69.5	69.2	59.6	-
Cycle-CLSWGAN [4]	66.8	-	58.6	70.3
LisGAN [12]	70.6	70.4*	58.8	69.9
f-VAEGAN-D2 [30]	71.1	-	61.0	67.7
RELATION NET [22]	68.2	64.2	55.6	78.5*
<b>MTN (Ours)</b>	<b>74.3</b>	<b>72.8</b>	<b>71.6</b>	<b>87.0</b>

CUB from 61.0% to 71.6%, and on FLO from 78.5% to 87.0%, i.e., all quite significant. We also observe that the improvement margins on fine-grained datasets are larger than those on the coarse-grained datasets, which indicates that the proposed approach transfers more discriminative information to distinguish categories. Another observation is that the classification performances of generative approaches are much better than those of discriminative approaches. This may be due to the following two facts. On one hand, the generative approaches alleviate the “hubness” issue in the zero-shot learning task. On the other hand, all the generative approaches are nonlinear approaches that handle better complicated semantic relations between the visual features and class semantic features. Compared with the other episode-based approach RELATION NET [22], our MTN achieves significant improvements on four datasets, which indicates our mimetic strategy captures more transfer knowledge than learning metric space strategy.

#### 4.2.2 Results on generalized ZSL.

Under the generalized ZSL setting, the test instances are classified into the joint label space spanned by both seen and unseen classes. Therefore, we follow the standard protocol proposed in [29] to evaluate the approaches with both seen class accuracy  $s$  and unseen class accuracy  $u$ , as well as their harmonic mean  $H$ . We provide the generalized ZSL results of our MTN and twelve competitors in Table 3.

The generalized ZSL results in Table 3 show that our MTN significantly improves the  $H$  measure against the state-of-the-art with a large margin on AwA1, CUB, and

FLO datasets and achieves second best performance in the  $H$  measure on the AwA2 dataset, which is only 1.6% inferior to the best result. On the AwA1, MTN obtains 68.1% in the  $H$  measure, significantly improving the second-best performance 63.5%, on the CUB dataset, it improves the state-of-the-art result from 53.6% to 58.1%, and on the FLO it achieves 77.9%, obtaining 9.6% gains against the state-of-the-art. The performance improvements verify the effectiveness of the proposed MTN on the generalized ZSL task.

We also observe that the seen classification accuracy  $s$  is much better than unseen classification accuracy  $u$ , even though the number of seen test instances are larger than that of unseen test instances on four datasets except for the AwA2 dataset (see Table 1), which indicates that the unseen test instances tend to be incorrectly classified into the seen classes. This classification shift issue is common across all the existing approaches. From the results, we observe that the generative approaches alleviate this shift issue to some extent. However, those approaches balance the differences between the seen class accuracy and the unseen class accuracy via decreasing the seen class accuracy while improving the unseen class accuracy. For example, though SE-ZSL [10] achieves best in  $H$  measure on AwA2 datasets. its seen class accuracy degrades significantly compared with the best  $s$  result, which is not desirable in practice. In contrast, our MTN improves the unseen class accuracy while maintaining the seen class accuracy, which substantially boosts the harmonic mean  $H$ .

Another observation is that the classification performances on the AwA2 dataset are inferior to those on the AwA1 dataset. This is due to that AwA2 contains more visual images as well as test instances than AwA1. Besides, for the fine-grained datasets, the classification performances on the FLO dataset are better than those on the CUB dataset, this is due to that CUB is a more challenging dataset that consists of more categories than FLO.

### 4.3. Further Analysis

In this section, we conduct further analysis to investigate the effect of the number of test classes per episode and the distance metric on the classification performance of the proposed MTN.

#### 4.3.1 Effect of test episode-based paradigm.

In the first experiment, we evaluate how the number of selected mimetic unseen classes affect the performances of the proposed approach on different datasets. To do so, we vary the number of selected mimetic unseen classes from 0 to 10 in intervals of 5. It should be noted that the case where the number of selected mimetic unseen classes equaling 0 indicates the approach without the episode-based training paradigm and the optimization process degenerates to the

Table 3. Performance (in %) comparisons in the generalized settings with unseen accuracy, seen accuracy, and their harmonic mean. \* indicates the result obtained by ourselves with the codes released by the authors.

Method	AwA1			AwA2			CUB			FLO		
	u	s	H	u	s	H	u	s	H	u	s	H
DEWISE [6]	13.4	68.7	22.4	17.1	74.7	27.8	23.8	53.0	32.8	9.9	44.2	16.2
ALE [1]	16.8	76.1	27.5	14.0	81.8	23.9	23.7	<b>62.8</b>	34.4	13.3	61.6	21.9
ESZSL [18]	2.4	70.1	4.6	5.9	77.8	11.0	12.6	63.8	21.0	11.4	56.8	19.0
SJE [2]	11.3	74.6	19.6	8.0	73.9	14.4	23.5	59.2	33.6	13.9	47.6	21.5
LATEM [27]	7.3	71.7	13.3	11.5	77.3	20.0	15.2	57.3	24.0	6.6	47.6	11.5
GAZSL [35]	29.6	84.2	43.8	35.4	86.9	50.3	31.7	61.3	41.8	28.1	77.4	41.2
CLSWGAN [28]	57.9	61.4	59.6	56.1	65.5	60.4	43.7	57.7	49.7	59.0	73.9	65.6
Cycle-CLSWGAN [4]	56.9	64.0	60.2	-	-	-	45.7	61.0	52.3	59.2	72.5	65.1
SE-ZSL [10]	56.3	67.8	61.5	<b>58.3</b>	68.1	<b>62.8</b>	41.5	53.3	46.7	-	-	-
LisGAN [12]	52.6	76.3	62.3	47.0*	77.6*	58.5*	46.5	57.9	51.6	57.7	83.8	68.3
f-VAEGAN-D2 [30]	57.6	70.6	63.5	-	-	-	48.4	60.1	53.6	56.8	74.9	64.6
RELATION NET [22]	31.4	<b>91.3</b>	46.7	30.0	<b>93.4</b>	45.3	38.1	61.1	47.0	50.8*	<b>88.5*</b>	64.5*
MTN (Ours)	<b>56.3</b>	86.2	<b>68.1</b>	47.9	84.6	61.2	<b>54.9</b>	61.8	<b>58.1</b>	<b>73.4</b>	82.9	<b>77.9</b>

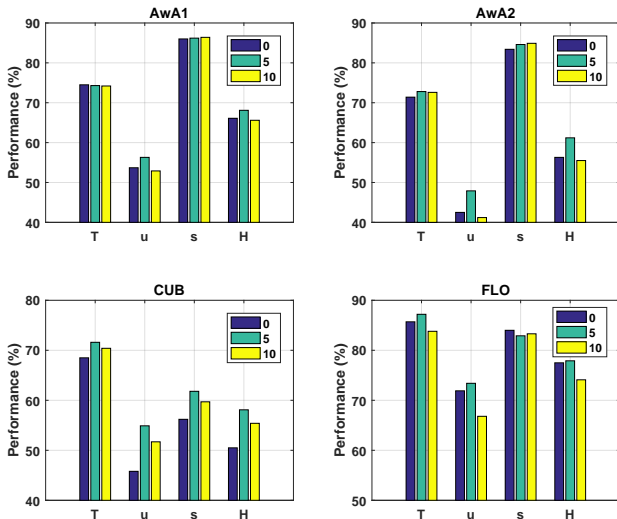


Figure 4. Traditional ZSL and generalized ZSL performances on four datasets with different numbers of test classes in per episode.

traditional batch-based training strategy.

According to the results in Fig. 4, we observe that the performances with  $M = 5$  are superior to those with  $M = 0$  on all datasets under different evaluation metrics except for the  $s$  on the FLO dataset, which verifies the effectiveness of the proposed episode-based strategy. Besides, we observe that the performances with  $M = 10$  are inferior to those with  $M = 5$ , which maybe due to that with the increase of the mimetic unseen classes, less training classes are left for training the visual-semantic alignment model, leading to unsatisfied initialization for the prediction of the mimetic unseen classes. Another observation is that different datasets differ greatly in the performance trend. For example, AwA1 and AwA2 have a similar trend because they come from the same categories. On both AwA1 and AwA2

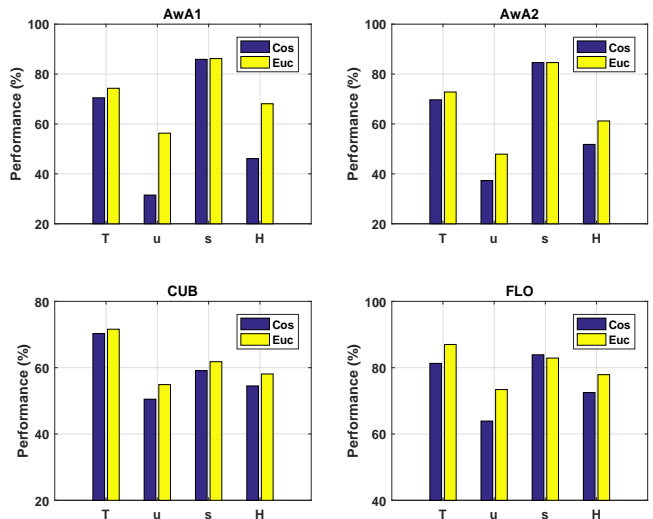


Figure 5. Tradition ZSL and generalized ZSL results with Euclidean distance (short for Euc) and Cosine distance (short for Cos) on four datasets.

datasets, the episode-based paradigm brings little impacts on the  $T$ , which indicates that the well-designed multi-modal interaction model is discriminative on the coarse-grained datasets if the predicted label space is restrict to the unseen categories. However, on the CUB dataset, the episode-based paradigm improves the performances significantly under different evaluation metrics, which verifies that the proposed episode-based paradigm works well on the fine-grained datasets. Compared with the results on the CUB dataset, the improvements on the FLO are less impressive since the FLO dataset consists of less categories than the CUB dataset.

### 4.3.2 Effect of distance metric.

In the second experiment, we investigate how the distance metric affects the classification performance on four datasets. In Fig. 5, we compare Cosine vs. Euclidean distance under different metrics on four datasets. We observe that the performances obtained in the Euclidean space significantly outperform those obtained in the Cosine space, indicating that the Euclidean distance is more suitable in our approach since the Cosine distance is not a Bregman divergence.

## 5. Conclusion

In this paper, we have proposed a meta-transfer network to learn to address zero-shot learning. The basic training framework is based on an episode-based paradigm, where each episode mimics a zero-shot learning task on the seen categories. The learner is a well-designed visual-semantic interaction model to efficiently align cross-modality semantic consistency and capture the discriminative information. The meta-learner fine-tunes the parameters of the learner by minimizing the differences between the prediction and the ground-truth labels of the mimetic unseen data. By training extensive episodes, the model accumulates a wealth of experiences on addressing classification scenarios where the training and the test classes are disjoint. The experimental results on four datasets demonstrate that the proposed model achieves the state-of-the-art on both traditional ZSL and generalized ZSL tasks and beats the other competitors on the fine-grained datasets with a large margin.

## References

- [1] Zeynep Akata, Florent Perronnin, Zaid Harchaoui, and Cordelia Schmid. Label-embedding for attribute-based classification. In *CVPR*, pages 819–826, 2013.
- [2] Zeynep Akata, Scott Reed, Daniel Walter, Honglak Lee, and Bernt Schiele. Evaluation of output embeddings for fine-grained image classification. In *CVPR*, pages 2927–2936, 2015.
- [3] Martin Arjovsky, Soumith Chintala, and Léon Bottou. Wasserstein gan. In *ICML*, 2017.
- [4] Rafael Felix, Vijay BG Kumar, Ian Reid, and Gustavo Carneiro. Multi-modal cycle-consistent generalized zero-shot learning. In *ECCV*, pages 21–37, 2018.
- [5] Chelsea Finn, Pieter Abbeel, and Sergey Levine. Model-agnostic meta-learning for fast adaptation of deep networks. In *ICML*, pages 1126–1135, 2017.
- [6] Andrea Frome, Greg S Corrado, Jon Shlens, Samy Bengio, Jeff Dean, Tomas Mikolov, et al. Devise: A deep visual-semantic embedding model. In *NeurIPS*, pages 2121–2129, 2013.
- [7] Ian Goodfellow, Jean Pouget-Abadie, Mehdi Mirza, Bing Xu, David Warde-Farley, Sherjil Ozair, Aaron Courville, and Yoshua Bengio. Generative adversarial nets. In *NeurIPS*, pages 2672–2680, 2014.
- [8] Ishaan Gulrajani, Faruk Ahmed, Martin Arjovsky, Vincent Dumoulin, and Aaron C Courville. Improved training of wasserstein gans. In *NeurIPS*, pages 5767–5777, 2017.
- [9] Diederik P Kingma and Max Welling. Autoencoding variational bayes. In *ICLR*, 2014.
- [10] Vinay Kumar Verma, Gundeep Arora, Ashish Mishra, and Piyush Rai. Generalized zero-shot learning via synthesized examples. In *CVPR*, pages 4281–4289, 2018.
- [11] Christoph H Lampert, Hannes Nickisch, and Stefan Harmeling. Learning to detect unseen object classes by between-class attribute transfer. In *CVPR*, pages 951–958, 2009.
- [12] Jingjing Li, Mengmeng Jin, Ke Lu, Zhengming Ding, Lei Zhu, and Zi Huang. Leveraging the invariant side of generative zero-shot learning. In *CVPR*, 2019.
- [13] Maria-Elena Nilsback and Andrew Zisserman. Automated flower classification over a large number of classes. In *ICCVGI*, pages 722–729, 2008.
- [14] Mark Palatucci, Dean Pomerleau, Geoffrey E Hinton, and Tom M Mitchell. Zero-shot learning with semantic output codes. In *NerIPS*, pages 1410–1418, 2009.
- [15] Hang Qi, Matthew Brown, and David G Lowe. Low-shot learning with imprinted weights. In *CVPR*, pages 5822–5830, 2018.
- [16] Sachin Ravi and Hugo Larochelle. Optimization as a model for few-shot learning. In *ICLR*, 2017.
- [17] Scott Reed, Zeynep Akata, Honglak Lee, and Bernt Schiele. Learning deep representations of fine-grained visual descriptions. In *CVPR*, pages 49–58, 2016.
- [18] Bernardino Romera-Paredes and Philip Torr. An embarrassingly simple approach to zero-shot learning. In *ICML*, pages 2152–2161, 2015.
- [19] Yutaro Shigeto, Ikumi Suzuki, Kazuo Hara, Masashi Shimbo, and Yuji Matsumoto. Ridge regression, hubness, and zero-shot learning. In *ECML&KDD*, pages 135–151, 2015.
- [20] Jake Snell, Kevin Swersky, and Richard Zemel. Prototypical networks for few-shot learning. In *NeurIPS*, pages 4077–4087, 2017.
- [21] Richard Socher, Milind Ganjoo, Christopher D Manning, and Andrew Ng. Zero-shot learning through cross-modal transfer. In *NerIPS*, pages 935–943, 2013.
- [22] Flood Sung, Yongxin Yang, Li Zhang, Tao Xiang, Philip H S Torr, and Timothy M Hospedales. Learning to compare: Relation network for few-shot learning. In *CVPR*, pages 1199–1208, 2018.
- [23] Oriol Vinyals, Charles Blundell, Timothy Lillicrap, Daan Wierstra, et al. Matching networks for one shot learning. In *NerIPS*, pages 3630–3638, 2016.
- [24] Catherine Wah, Steve Branson, Peter Welinder, Pietro Perona, and Serge Belongie. The caltech-ucsd birds-200-2011 dataset. 2011.
- [25] Wenlin Wang, Yunchen Pu, Vinay Kumar Verma, Kai Fan, Yizhe Zhang, Changyou Chen, Piyush Rai, and Lawrence Carin. Zero-shot learning via class-conditioned deep generative models. In *AAAI*, 2018.
- [26] Xiu-Shen Wei, Peng Wang, Lingqiao Liu, Chunhua Shen, and Jianxin Wu. Piecewise classifier mappings: Learning



- fine-grained learners for novel categories with few examples. *IEEE TIP*, 2019.
- [27] Yongqin Xian, Zeynep Akata, Gaurav Sharma, Quynh Nguyen, Matthias Hein, and Bernt Schiele. Latent embeddings for zero-shot classification. In *CVPR*, pages 69–77, 2016.
- [28] Yongqin Xian, Tobias Lorenz, Bernt Schiele, and Zeynep Akata. Feature generating networks for zero-shot learning. In *CVPR*, pages 5542–5551, 2018.
- [29] Yongqin Xian, Bernt Schiele, and Zeynep Akata. Zero-shot learning-the good, the bad and the ugly. In *CVPR*, pages 4582–4591, 2017.
- [30] Yongqin Xian, Saurabh Sharma, Bernt Schiele, and Zeynep Akata. f-vaegan-d2: A feature generating framework for any-shot learning. In *CVPR*, pages 10275–10284, 2019.
- [31] Yunlong Yu, Zhong Ji, Yanwei Fu, Jichang Guo, Yanwei Pang, and Zhongfei (Mark) Zhang. Stacked semantics-guided attention model for fine-grained zero-shot learning. In *NeurIPS*, pages 5995–6004, 2018.
- [32] Yunlong Yu, Zhong Ji, Jichang Guo, and Zhongfei Zhang. Zero-shot learning via latent space encoding. *IEEE Transactions on Cybernetics*, 49(10):3755–3766, 2019.
- [33] Yunlong Yu, Zhong Ji, Xi Li, Jichang Guo, Zhongfei Zhang, Haibin Ling, and Fei Wu. Transductive zero-shot learning with a self-training dictionary approach. *IEEE Transactions on Cybernetics*, 48(10):2908–2919, 2018.
- [34] Li Zhang, Tao Xiang, and Shaogang Gong. Learning a deep embedding model for zero-shot learning. In *CVPR*, pages 2021–2030, 2017.
- [35] Yizhe Zhu, Mohamed Elhoseiny, Bingchen Liu, Xi Peng, and Ahmed Elgammal. A generative adversarial approach for zero-shot learning from noisy texts. In *CVPR*, pages 1004–1013, 2018.